

Are your MRI contrast agents cost-effective?

Learn more about generic Gadolinium-Based Contrast Agents.



FRESENIUS  
KABI

caring for life

**AJNR**

## **Applications of a Novel Microangioscope for Neuroendovascular Intervention**












V.M. Srinivasan, T.T. Lazaro, A. Srivatsan, P. Cooper, M. Phillips, R. Garcia, S.R. Chen, J.N. Johnson, J.-K. Burkhardt, D.E. Collins and P. Kan

This information is current as of April 20, 2024.

*AJNR Am J Neuroradiol* published online 24 December 2020

<http://www.ajnr.org/content/early/2020/12/24/ajnr.A6900>

# Applications of a Novel Microangiogram for Neuroendovascular Intervention

 V.M. Srinivasan,  T.T. Lazaro,  A. Srivatsan,  P. Cooper,  M. Phillips,  R. Garcia,  S.R. Chen,  J.N. Johnson,  J.-K. Burkhardt,  D.E. Collins, and  P. Kan



## ABSTRACT

**BACKGROUND AND PURPOSE:** Visualization in neuroendovascular intervention currently relies on biplanar fluoroscopy and contrast administration. With the advent of endoscopy, direct visualization of the intracranial intravascular space has become possible with microangiograms. We analyzed the efficacy of our novel microangiogram to enable direct observation and inspection of the cerebrovasculature, complementary to a standard fluoroscopic technique.

**MATERIALS AND METHODS:** Iterations of microangiograms were systematically evaluated for use in neurodiagnostics and neurointerventions in both live animal and human cadaveric models. Imaging quality, trackability, and navigability were assessed. Diagnostic procedures assessed included clot identification and differentiation, plaque identification, inspection for vessel wall injury, and assessment of stent apposition. Interventions performed included angiogram-assisted stent-retriever thrombectomy, clot aspiration, and coil embolization.

**RESULTS:** The microangiogram was found helpful in both diagnosis and interventions by independent evaluators. Mean ratings of the imaging quality on a 5-point scale ranged from 3.0 (clot identification) to 4.7 (Pipeline follow-up). Mean ratings for clinical utility ranged from 3.0 (aspiration thrombectomy) to 4.7 (aneurysm treatment by coil embolization and WEB device).

**CONCLUSIONS:** This fiber optic microangiogram can safely navigate and visualize the intravascular space in human cadaveric and in vivo animal models with satisfactory resolution. It has potential value in diagnostic and neurointerventional applications.

**ABBREVIATIONS:** ICAD = intracranial atherosclerotic disease; IVUS = intravascular ultrasound; OCT = optical coherence tomography

Modern endovascular technique relies on fluoroscopy and contrast agents to guide visualization of the vasculature and deploy interventional devices. Even advanced techniques using conebeam CT are limited to this type of indirect visualization of the intravascular space—that is, that the operator cannot see what is not shown by the contrast or inherent radio-opacity. Matched with challenging anatomy, this indirect visualization

can lead to suboptimal clinical and radiologic outcomes, as well as complications.<sup>1,2</sup>

Methods of direct intravascular visualization have been studied for neuroendovascular application, namely, intravascular ultrasound (IVUS) and optical coherence tomography (OCT). IVUS uses an ultrasound microcatheter and provides real-time cross-sectional images from inside the artery; it has been studied in stent placement for cervical atherosclerotic disease.<sup>3,4</sup>

OCT involves using a fiber optic wire that emits near-infrared light that produces a signal based on the scattered or reflected light off the surrounding tissue and has been used to evaluate atherosclerotic disease and flow-diversion device placement.<sup>5-7</sup> Nonetheless, both IVUS and OCT face notable challenges because they offer neither direct visualization of intravascular pathology nor the miniaturization necessary to be compatible with the intracranial vasculature.

Prior studies of “angiograms” (intravascular endoscope)<sup>8-10</sup> have focused on larger vessels (cervical carotid artery). These were 7F and 5F guide catheters, again too large and inflexible for intracranial vessels.<sup>11</sup>


Received July 6, 2020; accepted after revision September 5.

From the Department of Neurosurgery (V.M.S., T.T.L., A.S., R.G., J.N.J., J.-K.B., P.K.) and Center for Comparative Medicine (D.E.C.), Baylor College of Medicine, Houston, Texas; Vena Medical (P.C., M.P.), Kitchener, Ontario, Canada; and Department of Interventional Radiology (S.R.C.), The MD Anderson Cancer Center, Houston, Texas.

Funding for the experiments was from Vena Medical, the manufacturer of the devices used in this study.

Paper previously presented as an oral presentation for an “Innovator of the Year” award at: Congress of Neurological Surgeons Annual Meeting, October 19–23, 2019; San Francisco, California.

Please address correspondence to Peter Kan, MD, Department of Neurosurgery, Baylor College of Medicine, 7200 Cambridge St, Suite 9B, Houston, TX 77030; e-mail: ptkan@utmb.edu; @PeterKa80460001

 Indicates article with online supplemental data.

<http://dx.doi.org/10.3174/ajnr.A6900>

Our group has recently described the development of a novel microangiogram for neurointerventional application.<sup>11</sup> The goal of this device is to provide direct, in vivo intravascular imaging of pathology and neurointerventional devices to augment the view by traditional fluoroscopy. In initial development, the device was tested in an in vivo porcine model, and several adjustments were made.

In this follow-up study, we aimed to develop this high-resolution microangiogram for clinical application in the human cerebrovasculature. The goals were to assess the compatibility of the device with the human cerebrovasculature (based on the interaction with the delivery system and flexibility) and its diagnostic utility and validity in assisting neurointerventions in animal models (based partially on image quality/resolution).

## MATERIALS AND METHODS

The study was approved by the institutional animal care and use committee (AN-5442). Several prototype microangiograms, not yet commercially available, were used for intravascular visualization (Vena Medical). The development of the microangiogram and technologic background have been previously described.<sup>11</sup> The first aim of this study was to improve on the resolution, flexibility, depth of view, and ergonomics of the previous microangiogram.

As previously described, continuous high-flow irrigation (50 mL/min) was performed via a balloon guide catheter or balloon distal access catheter (not commercially available). The combination of flow arrest and irrigation allowed visualization up to 3 cm distal to the distal access catheter or guide catheter.<sup>11</sup>

Three independent evaluators assessed the image quality for diagnostic utility of the live camera feed and processed procedural videos. Compatibility with the human cerebrovasculature was assessed by a separate cadaver study. Finally, the perceived utility of the microangiogram for diagnostic and interventional applications was graded by the same 3 independent evaluators, again using live camera intraprocedural feed and processed operative videos from cadaver and animal experiments. Procedures were performed by a fellowship-trained neurointerventionalist, and assessments were performed independently by 3 other neurointerventionalists. Videos were assessed using a 5-point qualitative scale (1 = poor, nondiagnostic; 2 = limited diagnostic value; 3 = average, some restricted visibility; 4 = good quality, minimal restrictions on visibility; 5 = excellent) based on prior similar radiographic analysis.<sup>12</sup> The clinical utility for the interventions was rated on a similar-but-separate 5-point qualitative scale based on the added information and the likelihood of using the microangiogram in the clinical setting. A structured debriefing session was then conducted between the engineering team and the clinicians following each experiment to allow iterative improvement of the microangiogram.

Periprocedural animal care (porcine and rabbit) was provided by a veterinary team, according to previously published protocols.<sup>13</sup> On completion of the study, the animals were euthanized under anesthesia.

Red and white thrombi were prepared using autologous porcine blood. Red thrombi were prepared by mixing autologous blood with bovine thrombin. White thrombi were obtained after centrifuge separation of autologous whole blood. Thrombus

preparation and the model for large-vessel occlusion have been previously described.<sup>13</sup>

The cadaver model was a formalin-fixed whole body. Standard surgical exposure was performed of the cervical carotid artery, which was transected. The distal access catheter was placed within the arterial lumen, and a suture was placed to close the artery around the catheter.

Last, a fusiform aneurysm with intimal injury was created using a rabbit survival model, in which the right common carotid artery was exposed and a 1-cm segment was trapped with 2 aneurysm clips. Elastase (12.5 U; Worthington Biochemical) was injected into the isolated segment and incubated for 20 minutes before reperfusion. The rabbits underwent follow-up angiography 4 weeks later to assess the device and vessel again. Further details about animal research methodology (according to ARRIVE guidelines; <https://arriveguidelines.org/>) are described in the Online Supplemental Data.

Statistical analysis was performed in Excel (Microsoft) for typical descriptive statistics; mean ratings are displayed as mean [SD].

## RESULTS

### *Technologic Iterations and Improvement*

Since the first generation of the microangiogram, considerable effort has been made to improve the device in 4 major areas: resolution, flexibility, FOV, and depth of view. Resolution was improved by increasing the number of pixels from 1600 to 3000. This resulted in more resolving power. With this addition, the FOV also increased from 33.3° to 50°, which made it capable of capturing more of the intravascular environment.

Flexibility was the next important factor, especially for the application to the human cerebrovasculature. This was improved by thinning the image bundle, increasing flexibility by >50% and by selecting more malleable materials for the outer sheath. The overall outer diameter was reduced from 2.1F to 1.7F, increasing flexibility by >100%. In silicone model testing (not shown), the minimum bend radius was determined to be <3.1 mm, which was corroborated by the models tested here. Ultimately, these improvements resulted in a marked reduction in stiffness and allowed the device to traverse into the tortuous anatomy of the human cerebrovasculature. Finally, a greater depth of view was important to advance or retract the device.

Three-watt battery-powered LED light sources were used in our initial experiments, but these only illuminated surfaces within 3 mm of the tip of the device. The light source was upgraded to a L9000 LED Light Source (Stryker Endoscopy), improving the depth of view to between 5 and 10 mm. However, due to poor white balancing with this iteration, the final version included a Stryker X7000 Xenon Light Source (Stryker Endoscopy). This 300-watt xenon lamp provided a white light source with even greater illumination at the tip of the device. By improving the light source as well as the number of illuminating fibers, we were able to increase the light intensity by >20%, which ultimately allowed a greater depth of view.

Much of the focus has also been on improving the human factors associated with the use of the microangiogram. Moving from a battery-powered light source to a standard endoscopy

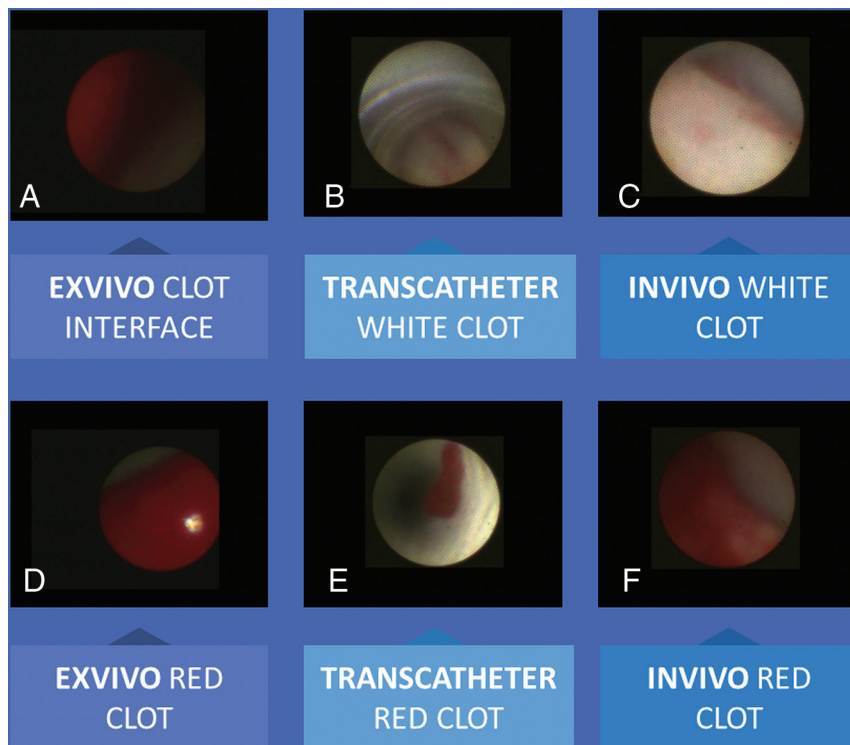


**FIG 1.** Clot identification and differentiation. A, Clot interface seen ex vivo with a red clot. A white clot is seen through the catheter (B) and in vivo in a porcine model (C). Red clots are seen clearly ex vivo (D), within the distal access catheter (E), and in vivo lodged in the porcine vessel (F).

light source meant that the light source did not need to be changed midway through a procedure. This feature naturally improved the workflow by extending the continuous viewing time of the camera. In addition, the display unit was changed from a cart-based one in which the physician must intermittently look away from the fluoroscope images to see the microangiographic images to an “integrated” display so that both fluoroscopic and angiographic images can be seen side by side on the Artis zeego monitor (Siemens) (Online Supplemental Data). The microangiographic also originally had a threaded attachment to the proximal assembly that was cumbersome and slow to couple. That was refined to a quick-disconnect system that takes 1 easy motion to replace the scope intraoperatively if necessary. Along with an increased working length of 150 cm and extended cables from the microangiographic to the control console, these improvements provide physicians and nurses with added flexibility and ease of operation. The overall advances between the first-generation and the current generation have resulted in a clinically acceptable device that can now be used to practically image the intravascular space (Online Supplemental Data).

#### **Diagnostic Utility: Clot Identification and Differentiation**

Autologous porcine blood clots were created and injected into the porcine external carotid circulation. Distinct clots (“red clot” or “white clot”) were made by separation of whole-blood

products to mimic the red cell-rich or fibrin-rich clots. The mean rating for clot identification by video and static images was 3.0 [SD, 1]. Clots were viewed in both ex vivo and in vivo settings. The clarity of the images was sufficient to differentiate the color of the clots as a proxy for their composition (Fig 1). The individual ratings are shown in the Table.

#### **Compatibility with Human Cerebrovasculature**

Because our initial proof-of-concept study<sup>11</sup> was in an animal model and prior studies with an angiographic had evaluated only up to the human cervical carotid artery, we expanded the angiography into the human intracranial vasculature using a cadaver model. After gaining access via the common carotid artery, the microangiographic was successfully navigated to the MCA with acceptable force within a distal access catheter using conventional angiography (Catalyst 5; Stryker Neurovascular). This deliverability was compared at the time of procedure with other deployed devices (stent retriever) and was comparable with the deployment of a stent retriever

in stiffness/tracking. At the most distal aspect, the microangiographic was positioned in the distal M1 to visualize the MCA bifurcation. No untoward events such as vessel dissection or perforation were noted.

#### **Diagnostic Utility: Carotid Disease and Intracranial Atherosclerotic Disease**

The mean rating for the carotid disease and intracranial atherosclerotic disease (ICAD) was 4.0 [SD, 1] in the human cadaver model. In the procedure, a plaque was noted in the proximal internal carotid artery, just past the carotid bifurcation (Online Supplemental Data). This was visualized clearly as a plaque via the microangiographic but was missed on subsequent conventional angiography. Going further distally into the intracranial circulation, we identified an intracranial plaque within the artery (Online Supplemental Data), which was also not visualized on subsequent angiography.

#### **Diagnostic Utility: Vessel Wall Injury**

In the rabbit model, a fusiform aneurysm was created by incubation of the arterial segment with elastase. The mean rating for the microangiographic video visualizing the diseased intima of this segment was 3.3 [SD, 1.2]. In this in vivo model, the differentiation of the intima between this segment and the normal segment proximally was seen as a luminal irregularity within the diseased segment. The irregularity was visualized by both angiography

## Ratings of microangiogram image quality and interventional utility

| Ratings                           | MD 1 | MD 2 | MD 3 | Mean |
|-----------------------------------|------|------|------|------|
| Image-quality rating <sup>a</sup> |      |      |      |      |
| Video clip                        |      |      |      |      |
| Diagnostic, cadaver carotid       | 3    | 4    | 5    | 4.0  |
| Diagnostic, clot identification   | 2    | 3    | 4    | 3.0  |
| Diagnostic, vessel wall injury    | 2    | 4    | 4    | 3.3  |
| Diagnostic, PED follow-up         | 4    | 5    | 5    | 4.7  |
| Diagnostic, PED initial           | 3    | 5    | 5    | 4.3  |
| Interventional, aspiration        | 2    | 4    | 3    | 3.0  |
| Interventional, stent retriever   | 3    | 4    | 3    | 3.3  |
| Interventional, coil embolization | 3    | 5    | 5    | 4.3  |
| Interventional, WEB deployment    | 2    | 5    | 3    | 3.3  |
| Utility rating <sup>a</sup>       |      |      |      |      |
| Interventional application        |      |      |      |      |
| Aspiration                        | 2    | 4    | 3    | 3.0  |
| Stent retriever                   | 3    | 4    | 3    | 3.3  |
| Coil embolization                 | 4    | 5    | 5    | 4.7  |
| WEB deployment                    | 4    | 5    | 5    | 4.7  |

**Note:**—MD indicates independent neurointerventionalist evaluator.

<sup>a</sup>One worst; 5 best. Image quality rating scale described first, followed by device interventional utility rating scale:

- 1) Poor, no diagnostic value; not useful at all for intervention.
- 2) Limited diagnostic value; minimally useful, just of research value/interest.
- 3) Average quality, of possible clinical utility; moderately useful, adds to procedure quality/safety.
- 4) Good quality, minimal restrictions on visibility, probably adds benefit beyond angiography; significantly useful, should strongly consider for this indication.
- 5) Excellent quality, adds benefit beyond angiography, could definitely use as an adjunct; extremely useful, would definitely use in most/all such procedures.

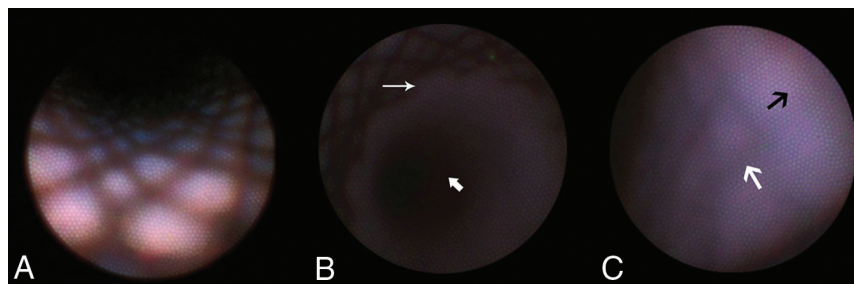


**FIG 2.** Visualization of a flow-diverting device by the microangiogram. *A*, The fine-woven mesh of the PED is seen. *B*, The interface between the PED and the distal vessel is seen (*thin arrow*), and the distal vessel is dark (*thick arrow*) and beyond the illumination of the microangiogram, giving depth perception. Thrombus formation is excluded, and good wall apposition is confirmed. *C*, After 1 month post-procedure, the device is partially endothelialized, with struts less visible (*medium white arrow*) and endothelium more prominent (*medium black arrow*).

and microangiogram (Online Supplemental Data: Video showing the diseased vessel in a rabbit model).

### Diagnostic Utility: Device Follow-Up

The fusiform aneurysm created in the prior experiment was then treated with flow diversion using the Pipeline Embolization Device (PED; Medtronic). The aneurysm and device were visualized immediately after device deployment to assess apposition (Fig 2A, -B) and 4 weeks later to assess endothelialization (Fig 2C). The mean rating for the new device placement was 4.3 [SD, 1.2], and the rating at follow-up was 4.7 [SD, 0.6]. Immediately after deployment, all stent tines and the interface between the stent and the normal vessel were well-visualized, and the ability to assess apposition was excellent. No thrombus was seen on the device surface. At follow-up, the same stent tines were visualized in only some areas, though less distinct, and in others, there was complete tissue coverage. We expect that this is secondary to the

desired endothelialization response, though it could also be a combination of fibrin deposition, smooth-muscle cell proliferation, or immune-cell attachment. This was deemed clinically relevant and useful in the follow-up of flow-diversion treatment by all independent evaluators.

### Interventional Utility: Stroke Thrombectomy

The feasibility and utility of the microangiogram as an adjunct in stroke thrombectomy was tested with the 2 main thrombectomy techniques: aspiration (A Direct Aspiration First Pass Technique [ADAPT] technique, Catalyst

5) and stent-retriever thrombectomy (Trevo, Stryker; and Embotrap II, Cerenovus) (Fig 3). Experiments were conducted across 3 porcine subjects. The mean rating for the ADAPT image quality was 3.0 [SD, 1], while the rating of visualization of the stent retriever thrombectomy was 3.3 [SD, 0.6]. The expected clinical utility was separately assessed, with a mean rating of 3.0 [SD, 1] for aspiration and 3.3 [SD, 0.6] for the stent retriever. These fall between 3, moderately useful, adds to procedure quality/safety and 4, significantly useful, should strongly consider for this indication.

In the aspiration experiment (3 attempts), a clot was delivered at a bifurcation and the microangiogram was positioned within the aspiration catheter as the pump was turned on. Distal fluid was seen flowing backward toward the camera. Once sufficient force was generated, the clot was aspirated toward the catheter tip and was “corked.” A “red out” was seen on the microangiogram as it was obscured by the face of the clot. A few seconds later, the



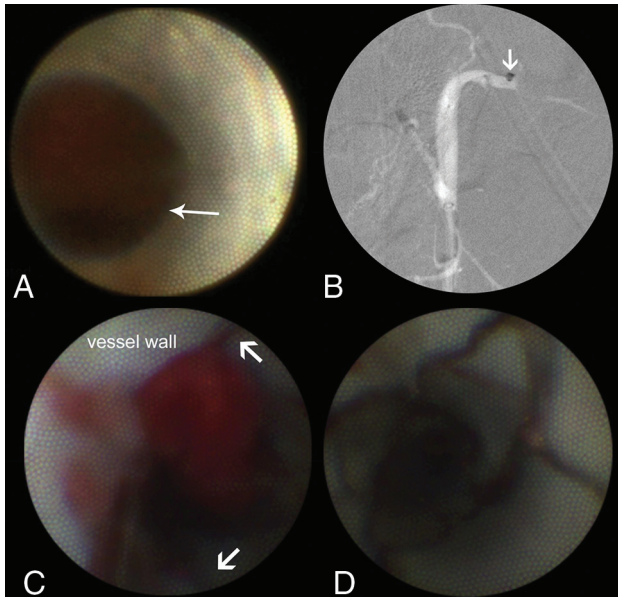


**FIG 3.** Visualization of mechanical thrombectomy. *A*, A clot is visualized by the microangiogram, and an aspiration catheter is positioned at the face of the clot. The interface between the artery and the clot is seen (*thin arrow*). *B*, Corresponding view on roadmap fluoroscopy shows the positioning of the aspiration catheter at the sharp cutoff point. *C*, A red thrombus is seen during removal by stent-retriever thrombectomy. *D*, The struts of the device can be clearly seen, as can the endothelium, with clear color differentiation (*thick arrows*).

clot was then ingested into the inner lumen of the aspiration catheter past the microangiogram, again giving clear visualization and confirming successful clot evacuation. The microangiogram then traversed outside the aspiration catheter and could visualize the newly recanalized segment. The camera was able to visualize small residual clot in the aspiration catheter, and this small clot was successfully aspirated by a second attempt (Online Supplemental Data: Data/Videos).

In the stent-retriever experiments (5 attempts), both Trevo and Embotrap II stent retriever thrombectomy was performed (Fig 3). In these cases, the tines and expansion of each device were clearly seen, regardless of their radio-opacity on fluoroscopy. Furthermore, the interface between the clot and the device could be visualized as the clot was retrieved. As in aspiration thrombectomy, the microangiogram could later adequately inspect the vessel after recanalization to confirm total revascularization.

All 8 vessels were recanalized after the first pass.

### **Interventional Utility: Aneurysm Treatment**

The feasibility and utility of the microangiogram as an adjunct in aneurysm treatment were tested with multiple devices, including coil embolization and intrasaccular flow disruption (Woven EndoBridge, WEB; MicroVention).

Aneurysm coiling was simulated in an *in vivo* porcine model. The microangiogram and the coiling microcatheter were simultaneously placed in a balloon guide catheter. The coils were deployed with the camera positioned at the origin of a vessel to simulate aneurysm coiling. The mean rating for this video was 4.3 [SD, 1.2]. The vessel origin, a surrogate of the aneurysm neck,

was well-visualized with the microangiogram. The distal vessel, however, as a surrogate for the aneurysm fundus, was better seen with conventional angiography. The mean rating for the clinical utility was 4.7 [SD, 1.2], which ranges between 4, significantly useful and 5, extremely useful, would definitely use in most/all such procedures.

Finally, an intrasaccular flow-disruption device (WEB), deployed at a vessel origin, was visualized with the microangiogram. The fine mesh of the device, very similar to the lattice of the PED, was visualized clearly, as was the interface between the device and the normal vessel as a surrogate for the aneurysm neck. The mean rating for this video was 3.3 [SD, 1.5]. The mean rating for the clinical utility was 4.7 [SD, 1.2].

## **DISCUSSION**

### **Shortcomings of Diagnostic Angiography**

DSA is the criterion standard for all modern neuroendovascular interventions but has notable disadvantages. Namely, high cumulative radiation doses, contrast usage, and poor visualization over bony anatomy limit its safety and utility. Furthermore, the proper visualization of devices with DSA relies largely on their radio-opacity. To this end, there has been interest in using IVUS and OCT as adjuncts to DSA. However, these methods have their own limitations, chiefly their cumbersome size and stiffness that limit safe neurovascular navigation.

### **From Angioscope to Microangiogram**

Angioscopy, as described in previous iterations, has been limited by visualization through blood *in vivo*, camera size, and image quality. In this study, we demonstrate the utility of a further-improved<sup>11</sup> high-resolution microangiogram. The miniaturization of the angioscopic technology is truly transformative and allows access into the distal intracranial vasculature (MCA bifurcation), as seen in the human cadaver experiments. In the iterative process used between our proof-of-concept study and the current version, the microangiogram optics have also been improved with better diagnostic quality. Specifically, improvement in the fiberoptic light source allowed better image resolution (increased image fibers) as well as intravascular illumination and depth of view (improved light source and increased illumination fibers). Additional improvements were also made to the flexibility and FOV of the device. Each successive iteration made for a quantitatively improved experience.

### **Diagnostic Applications**

Four discrete diagnostic applications were evaluated in this study: clot identification/differentiation, plaque identification, inspection of vessel wall injury, and flow-diverter apposition and endothelialization. The mean rating for these all reached above 3/5, qualifying for potential clinical benefit/use per the clinicians viewing the video.

The clot identification and differentiation have clear implications for mechanical thrombectomy. The ability to identify vessel wall injury and inspect the vessel wall surface is important for identifying subtle vascular dissection and differentiating vasculitis/vasospasm from diffuse atherosclerotic disease. These entities are often difficult to diagnose and differentiate on angiography,

and a microangioscope can clarify these diagnoses with direct visual inspection.

The uses of other intravascular visualization technologies (IVUS, OCT) have been studied in the context of flow-diversion follow-up.<sup>5,7</sup> In follow-up angiograms, usually obtained at 3- to 12-month intervals after aneurysm treatment, the neurointerventionalist evaluates parent artery patency, aneurysm occlusion, branch vessel patency, and in-stent stenosis. The goal of flow diversion is to achieve durable aneurysm occlusion by endothelialization of the stent across the aneurysm neck. However, complete aneurysm occlusion is only inferred by angiography in these experiments. In this study, the microangioscope was able to clearly identify the tissue response across the fine struts of the PED. With this technology, the successful treatment with a device can be monitored and could then dictate the necessary duration of antiplatelet therapy.

### **Interventional Applications: Stroke**

Various interventional applications were evaluated in this study, namely aneurysm treatment by several modalities (flow diversion with the PED, intrasaccular flow disruption with WEB, and aneurysm coiling) and stroke thrombectomy. In all interventions, device adjustments were made on the basis of real-time feedback to increase workflow and accuracy in a clinical setting. Overall, there is potential for assistance in thrombectomy as per the clinician ratings.

Practically, we envision the potential use of the microangioscope in stroke thrombectomy as an adjunct to the current treatment paradigm, which is meant to be performed swiftly<sup>14,15</sup> and with a high first-pass efficacy.<sup>16</sup> First, given the ability of the microangioscope to directly visualize and differentiate between white clot (high fibrin content, firm, recalcitrant) and red clot (high red blood cell content, softer, easier to remove), the optimal thrombectomy strategy could be chosen (aspiration versus stent retriever). If using aspiration, as in the case of a fibrin clot, the microangioscope can help identify when corking or when contact has been established and can identify any uncaptured/residual clot to be ingested. If using a stent retriever, in the case of a red thrombus, the microangioscope can visualize clot integration and identify residual, especially because some thrombi were not seen on conventional angiography. In this sense, the microangioscope shows up-close what was previously seen only in clear silicone flow models with simulated clots. The microangioscope practically gives us a “new set of eyes” in the angiography suite. Future translational research is certainly needed to corroborate some of the potential applications in our models and bring them to the angiography suite. Most important, these applications are limited by visualization just to the clot face (and not distal to it) and the flow-arrest requirement.

In another scenario, when there is re-occlusion, the microangioscope can be used to evaluate and differentiate between intracranial atherosclerosis and vasospasm/vasculitis and can help guide additional treatment such as rescue stent placement<sup>17</sup> in the case of ICAD or antispasmodics in case of vasospasm. From the perspective of carotid disease and stroke work-up, microangiography could potentially identify high-risk plaques (eg, thrombus or ulceration) in the setting of mild or normal-appearing

angiographic stenosis for patients with an otherwise unremarkable stroke work-up. This could be a key development in identifying the embolic source in this clinically challenging group of patients.<sup>18</sup>

### **Interventional Applications: Aneurysm Treatment**

The clinical utility ratings for the 2 aneurysm treatments (coil embolization and WEB deployment) were both very high, 4.7 [SD, 1.2]. In both of these treatments, visualization of the neck of the aneurysm is critical to ensure complete coverage and treatment and to prevent encroachment of the implant into the parent artery or branch artery. In standard fluoroscopy, oblique views are often needed to optimize visualization of the aneurysm neck and the normal artery. However, this can be challenging, depending on patient anatomy and aneurysm projection. Therefore, the ability of the microangioscope to directly visualize this critical area of the neck to ensure complete and safe device deployment is clinically significant.

### **Workflow**

The imagined workflow of angiography and microangiography is demonstrated in the Online Supplemental Data. These are complementary technologies. Generally, the microangioscope helps visualize proximal pathology and is somewhat limited distally, given the 3-cm tether from the balloon catheter. Thus, the distal anatomy is well-seen with angiography, which also provides a roadmap to go further with the microangioscope. Practically, this is similar to what neuroendoscopy has done in operative micro-neurosurgery; bringing the light source and visualization closer to the pathology has been revolutionary.<sup>19</sup> The ergonomics of where to position the operating instruments (microcatheter and microwire device) relative to the endoscope (microangioscope) are quite similar. Thus, in the aneurysm experiments, fluoroscopy and the microangioscope each had their own distinct advantages and were quite complementary. Overall, standard angiography demonstrates the distal aneurysm fundus and the walls well, whereas the neck of the aneurysm can be well-visualized with the microangioscope.

### **Future Directions**

This technology has myriad potential applications in neuroendovascular surgery and for both clinical and translational research to further our understanding of cerebrovascular diseases. For example, further quantitative studies should be performed to truly assess its value in microangioscope-assisted thrombectomy. In this study, we were able to visualize intracranial atherosclerotic disease in a cadaver experiment, but the results should be validated in further cadaveric and possibly in vivo human subjects. Our thrombectomy experiments suggest that direct visualization of thrombi could help the clinician with revascularization, and more quantitative revascularization outcomes should be tested.

Other types of vascular injury (intimal flaps/dissections, webs) can also be difficult to assess by angiography alone. In the assessment of its use in aneurysm treatment, these experiments were only a proof-of-concept and also deserve future study using well-established aneurysm models to explore the visualization of

device apposition, intraprocedural clot detection, and aneurysm neck healing with time.

### Limitations

The limitations of this technology were discussed in our prior proof-of-concept study.<sup>11</sup> Briefly, these are the inability to see distally beyond the pathology and the necessity for flow arrest. The duration of flow arrest could theoretically vary from procedure to procedure but certainly carries potential morbidity with the use of balloons and increased ischemic time during device manipulation.

The study itself additionally has limitations. This study has established the feasibility of its use in a human cadaver and a porcine model. The cadaver model had no flowing blood and did not require the ability to obtain intracranial flow arrest, and the external carotid artery of the porcine model had limited tortuosity and was of large diameter. Additionally, the outcome measures used to assess imaging quality and device compatibility are not validated.

### CONCLUSIONS

Current neuroendovascular imaging relies on fluoroscopy-based DSA. We used a recently developed fiber optic microangioscope to visualize the intravascular space in human cadaveric and in vivo animal models. In this series of experiments, we demonstrate its feasibility in diagnostic and neurointerventional applications. An independent rating of video capture suggested satisfactory visualization and potential utility, particularly in aneurysm embolization procedures. Further studies are needed to evaluate its potential in this and other applications, including diagnosis, device deployment, and treatment monitoring.

### ACKNOWLEDGMENT

We appreciate the excellent care of animal subjects by Dr Collins' veterinary team.

Disclosures: Tyler T. Lazaro—RELATED: Grant: Vena Medical, Comments: provided money to fund the experiments in this study. No money paid to the individual authors. Phillip Cooper—UNRELATED: Board Membership: Vena Medical, Comments: I am a board member at my startup, Vena Medical; Employment: Vena Medical; Stock/Stock Options: I own stock in my startup, Vena Medical; Travel/Accommodations/Meeting Expenses Unrelated to Activities Listed: Vena Medical pays for my travel. Michael Phillips—UNRELATED: Board Membership: Vena Medical, Comments: I am on the board of Vena Medical; Employment: Vena Medical; Patents (Planned, Pending or Issued): Vena Medical, Comments: I am an inventor of several pending patents assigned to Vena Medical; Stock/Stock Options: Vena Medical; Travel/Accommodations/Meeting Expenses Unrelated to Activities Listed: Vena Medical, Comments: travel and accommodations to conferences such as the World Live Neurovascular Conference, the Society of Neurointerventional Surgery, and so forth to represent Vena Medical. Jan-Karl Burkhardt—UNRELATED: Board Membership: Longeviti Neuro Solutions, Comments: Advisory Board member. Peter Kan—UNRELATED: Stock/Stock Options, Vena Medical.

### REFERENCES

1. Ketteler ER, Brown KR. Radiation exposure in endovascular procedures. *J Vasc Surg* 2011;53:355–38S [CrossRef Medline](#)
2. Wong JM, Ziewacz JE, Panchmatia JR, et al. Patterns in neurosurgical adverse events: endovascular neurosurgery. *Neurosurg Focus* 2012;33:E14 [CrossRef Medline](#)
3. Kan P, Mokin M, Abula AA, et al. Utility of intravascular ultrasound in intracranial and extracranial neurointerventions: experience at University at Buffalo Neurosurgery-Millard Fillmore Gates Circle Hospital. *Neurosurg Focus* 2012;32:E6 [CrossRef Medline](#)
4. Tobis JM, Mallery J, Mahon D, et al. Intravascular ultrasound imaging of human coronary arteries in vivo: analysis of tissue characterizations with comparison to in vitro histological specimens. *Circulation* 1991;83:913–26 [CrossRef Medline](#)
5. Caroff J, Tamura T, King RM, et al. Phosphorylcholine surface modified flow diverter associated with reduced intimal hyperplasia. *J Neurointerv Surg* 2018;10:1097–1101 [CrossRef Medline](#)
6. King RM, Marosfoi M, Caroff J, et al. High frequency optical coherence tomography assessment of homogenous neck coverage by intrasaccular devices predicts successful aneurysm occlusion. *J Neurointerv Surg* 2019;11:1150–54 [CrossRef Medline](#)
7. King RM, Brooks OW, Langan ET, et al. Communicating malapposition of flow diverters assessed with optical coherence tomography correlates with delayed aneurysm occlusion. *J Neurointerv Surg* 2018;10:693–97 [CrossRef Medline](#)
8. Tanemura H, Hatazaki S, Asakura F, et al. Angioscopic observation during carotid angioplasty with stent placement. *AJNR Am J Neuroradiol* 2005;26:1943–48 [Medline](#)
9. Savastano LE, Chaudhary N, Murga-Zamalloa C, et al. Diagnostic and interventional optical angioscopy in ex vivo carotid arteries. *Oper Neurosurg (Hagerstown)* 2017;13:36–46 [CrossRef Medline](#)
10. Savastano LE, Zhou Q, Smith A, et al. Multimodal laser-based angioscopy for structural, chemical and biological imaging of atherosclerosis. *Nat Biomed Eng* 2017;1:0023 [CrossRef Medline](#)
11. Lazaro T, Srinivasan VM, Cooper P, et al. A new set of eyes: development of a novel microangioscope for neurointerventional surgery. *J Neurointerv Surg* 2019;11:1036–39 [CrossRef Medline](#)
12. Srinivasan VM, Chintalapani G, Camstra KM, et al. Fast acquisition cone-beam computed tomography: initial experience with a 10 s protocol. *J Neurointerv Surg* 2018;10:916–20 [CrossRef Medline](#)
13. Srinivasan VM, Chen SR, Camstra KM, et al. Development of a recalcitrant, large clot burden, bifurcation occlusion model for mechanical thrombectomy. *Neurosurg Focus* 2017;42:E6 [CrossRef Medline](#)
14. Huang X, Cai Q, Xiao L, et al. Influence of procedure time on outcome and hemorrhagic transformation in stroke patients undergoing thrombectomy. *J Neurol* 2019;266:2560–70 [CrossRef Medline](#)
15. Saver JL, Goyal M, van der Lugt A, et al; HERMES Collaborators. Time to treatment with endovascular thrombectomy and outcomes from ischemic stroke: a meta-analysis. *JAMA* 2016;316:1279–88 [CrossRef Medline](#)
16. Zaidat OO, Castonguay AC, Linfante I, et al. First pass effect: a new measure for stroke thrombectomy devices. *Stroke* 2018;49:660–66 [CrossRef Medline](#)
17. Maingard J, Phan K, Lamanna A, et al. Rescue intracranial stenting after failed mechanical thrombectomy for acute ischemic stroke: a systematic review and meta-analysis. *World Neurosurg* 2019;132:e235–45 [CrossRef Medline](#)
18. Goyal M, Singh N, Marko M, et al. Embolic stroke of undetermined source and symptomatic nonstenotic carotid disease. *Stroke* 2020;51:1321–25 [CrossRef Medline](#)
19. Torres-Corzo JG, Rangel-Castilla L, Nakaji P. *Neuroendoscopic Surgery*. Thieme Publishers; 2016